AD_____

Award Number: DAMD17-01-1-0777

TITLE: Fundamental Patterns Underlying Neurotoxicity Revealed by
         DNA Microarray Expression Profiling

PRINCIPAL INVESTIGATOR: Karen L. O'Malley, Ph.D.

CONTRACTING ORGANIZATION: Washington University School of Medicine
                            St. Louis, Missouri   63110-1093

REPORT DATE: September 2004

TYPE OF REPORT: Final

PREPARED FOR: U.S. Army Medical Research and Materiel Command
                Fort Detrick, Maryland   21702-5012

DISTRIBUTION STATEMENT: Approved for Public Release;
                        Distribution Unlimited

The views, opinions and/or findings contained in this report are
those of the author(s) and should not be construed as an official
Department of the Army position, policy or decision unless so
designated by other documentation.

REPORT DOCUMENTATION PAGE

Form Approved
OMB No. 074-0188

1. AGENCY USE ONLY (Leave blank)	2. REPORT DATE September 2004	3. REPORT TYPE AND DATES COVERED Final (1 Sep 2001 – 31 Aug 2004)

4. TITLE AND SUBTITLE
Fundamental Patterns Underlying Neurotoxicity Revealed by DNA Microarray Expression Profiling

5. FUNDING NUMBERS
DAMD17-01-1-0777

6. AUTHOR(S)
Karen L. O'Malley, Ph.D.

7. PERFORMING ORGANIZATION NAME(S) AND ADDRESS(ES)
Washington University School of Medicine
St. Louis, Missouri 63110-1093

E-Mail: omalleyk@pcg.wustl.edu

8. PERFORMING ORGANIZATION REPORT NUMBER

9. SPONSORING / MONITORING AGENCY NAME(S) AND ADDRESS(ES)

U.S. Army Medical Research and Materiel Command
Fort Detrick, Maryland 21702-5012

10. SPONSORING / MONITORING AGENCY REPORT NUMBER

11. SUPPLEMENTARY NOTES
Original contains color plates: All DTIC reproductions will be in black and white.

12a. DISTRIBUTION / AVAILABILITY STATEMENT
Approved for Public Release; Distribution Unlimited

12b. DISTRIBUTION CODE

13. ABSTRACT (Maximum 200 Words)

The selective neurotoxins 1-methyl-4-phenylpyridinium (MPP^+) and 6-hydroxydopamine (6-OHDA) have been widely used to generate animal models of Parkinson's disease (PD). To understand the genetic events associated with these neurotoxins, microarray technology served to monitor differences in gene expression patterns in normal versus pathological conditions. Microarray analysis of RNA isolated from toxin treated samples revealed that the stress-induced transcription factor CHOP was dramatically up regulated by both toxins. 6-OHDA also induced a large number of genes involved in endoplasmic reticulum (ER) stress and unfolded protein response (UPR) such as ER chaperones and elements of the ubiquitin-proteasome system. RT-PCR, Western blotting, and immunocytochemical approaches were used to quantify and temporally order the UPR pathways involved in neurotoxin-induced cell death. 6-OHDA, but not MPP^+, significantly increased hallmarks of UPR such as BiP, c-jun, and processed Xbp1 mRNA. Both toxins increased the phosphorylation of UPR proteins, PERK and eIF2α, but only 6-OHDA increased phosphorylation of c-jun. Thus, 6-OHDA triggers multiple pathways associated with UPR, whereas MPP^+ exhibits a more restricted response. 6-OHDA induced similar responses in primary dopaminergic neurons. These experiments will help clarify the molecular mechanisms associated with 6-OHDA and MPP^+ toxicity and might aid in developing novel therapeutic avenues relevant to PD.

14. SUBJECT TERMS
MPP+, 5-OHDA; neurotoxicity; gene expression profiling; DNA microarray

15. NUMBER OF PAGES
22

16. PRICE CODE

17. SECURITY CLASSIFICATION OF REPORT Unclassified	18. SECURITY CLASSIFICATION OF THIS PAGE Unclassified	19. SECURITY CLASSIFICATION OF ABSTRACT Unclassified	20. LIMITATION OF ABSTRACT Unlimited

Table of Contents

Introduction

The selective neurotoxins 1-methyl-1,2,3,6-tetrahydropyridine (MPTP) and 6-hydroxydopamine (6-OHDA) have been widely used to generate animal models of Parkinson's disease (PD). To understand and order the genetic events associated with these neurotoxins, DNA microarray technology was used to monitor differences in gene expression patterns in normal versus pathological conditions. Eleven thousand murine genes and expressed sequence tags were screened to determine changes in gene expression caused by MPP+, the active metabolite of MPTP, and 6-OHDA in a mouse CNS dopaminergic cell line. Examining a time point at which cells treated with either toxin were committed to die (9 hours) led to the identification of numerous genes associated with ER stress/UPR (Holtz and O'Malley, 2003). Because temporal changes in gene expression patterns would be expected to occur, two earlier time points were also examined. Microarray analysis of RNA collected from three and six hour time points following 6-OHDA treatment was combined with data mining and clustering techniques, to identify distinct functional subgroups of genes. Notably, stress-induced transcription factors such as ATF3, ATF4, CHOP, and C/EBPß were robustly upregulated yet exhibited unique kinetic patterns. Genes involved in the synthesis and modification of proteins (various tRNA synthetases), protein degradation (e.g. ubiquitin, Herpud1, Sqstm1), and oxidative stress (Hmox1, Por) could be subgrouped into distinct kinetic profiles as well. Real time PCR and/or two-dimensional electrophoresis combined with Western blotting validated data derived from microarray analyses (Holtz et al., 2004a). Subsequent studies showed that 6-OHDA-mediated cell death in dopaminergic cells proceeds via ROS-dependent UPR up-regulation that leads to an interaction with the intrinsic mitochondrial pathway and downstream caspase activation (Holtz et al., 2004b). Taken together these data support the notion that oxidative stress and protein dysfunction play a role in PD as well as provide a time course for many of the molecular events associated with MPP$^+$ and 6-OHDA neurotoxicity.

Body

A.   Does the neurotoxin MPP$^+$ differentially regulate sets of genes?

As described in previous reports, MN9D cells were plated at a density of 200,000 cells/well in six-well plates. After three days, cells were treated with 50 µM MPP$^+$, or left untreated for control comparisons. Total RNA was isolated after 9 hours of toxin treatment using an RNeasy kit (Qiagen, Valencia, CA) according to the manufacturer's protocol. Equal amounts of total RNA from three independent experiments were pooled for each GeneChip hybridization. A minimum of 20 µg/sample of total RNA was sent to the Alvin J. Siteman Cancer Center GeneChip Core Facility (Washington University, St. Louis, MO) for generation of labeled cRNA target and hybridization against Affymetrix Murine Genome U74Av2 GeneChip arrays (Santa Clara, CA) using standard protocols (pathbox.wustl.edu/~mgacore/protocols.htm). Data were analyzed using Affymetrix Microarray Suite version 5.0. Data mining was performed using Spotfire Decision Site for Functional Genomics (Somerville, MA). For those transcripts designated both "present" and "increasing" by the software, a threshold of a signal log$_2$ ratio of 0.5 (~1.5-fold change) was set. Transcripts for which signal was less than 3% of the maximum signal were filtered out.

Out of the approximately 12,000 genes and ESTs represented on the MG-U74Av2 GeneChip, 4,304 (~35% of total) were defined as "present" by the microarray analysis software for MPP$^+$-treated samples. Transcripts were subsequently grouped by individual toxin treatment or by

both 6-OHDA and MPP$^+$. As presented in the previous report and included in the attached paper (Holtz and O'Malley, 2003), 59 transcripts increased in response to MPP$^+$ whereas 34 transcripts were decreased. Both neurotoxins induced a number of the same transcripts, with 43 of the 59 transcripts induced by MPP$^+$ also induced by 6-OHDA. These included genes involved in cell cycle and/or differentiation, signaling, stress, and transcription factors, indicating possible common cell death mechanisms. These results together with real time PCR and Western blot confirmation led us to propose that MPP$^+$ specifically attenuates protein translation within the ER stress/Unfolded Protein Response (UPR)-mediated cell death pathway.

We have subsequently examined microarray data derived from a single experiment at earlier time points (3, 6 hours). Using the threshold set in the previous experiment, it would not appear that any additional transcripts are activated at those time points. It may be, however, that by the time we have completed three independent microarray assessments at the earlier time points that data variability will be minimized such that small but significant transcriptional changes can be identified within this data set. This work is still in progress.

B.   Does the neurotoxin 6-OHDA differentially regulate sets of genes?

Microarray experiments described in previous reports and in Holtz and O'Malley (2003) revealed that 6-OHDA treatment increased the expression of many genes associated with cellular stress. As the prior studies looked only at a 9-hour end point, the latest time that macromolecular synthesis inhibitors could block cell death, subsequent studies were directed at establishing earlier hierarchical changes. RNAs prepared from untreated control, 3, and 6-hour 6-OHDA-treated cells were subjected to microarray analysis as described above. Data from these experiments were combined with information from our prior 9-hour time point to identify changes, generate expression profiles of transcriptional differences over time, and to group genes according to their profiles. Of the ~12,000 genes present on the GeneChip, the number of genes that met the criteria for increasing over control was 128 at 3 hours, 236 at 6 hours, and 239 at 9 hours. Of the 128 genes increased at 3 hours, 95 were in common with those increasing at 6 hours, and 53 were in common with the transcripts increasing at 9 hours. Of the 236 genes that were increasing at 6 hours, 113 were in common with those increasing at 9 hours. Of the 53 transcripts that were increased at both 3 and 9 hours, 51 were also increased at 6 hours. Thus, all but two genes increased at 3 and 9 hours were also increased at 6 hours (Table 1).

TABLE 1

Table 1. List of 48 transcripts increased by 6-OHDA over untreated control after 3, 6, and 9 hours.

Gene Symbol	Gene Name	Fold Induction		
		3hr	6hr	9hr
CHOP/Ddit3	DNA-damage inducible transcript 3	4.6	7.5	64
Hmox1	heme oxygenase-1	2.1	4.6	3.5
Sqstm1	sequestosome 1	2.1	4.6	8
Ubc	ubiquitin C	1.5	1.4	2.1
Sars1	seryl-aminoacyl-tRNA synthetase 1	1.4	1.9	2

Gene	Description			
Erdr1	erythroid differentiation regulator 1	1.4	2	1.9
Por	P450 (cytochrome) oxidoreductase	1.4	1.7	2
Myd116	myeloid differentiation primary response gene 116	1.7	3.5	3.5
Nupr1	nuclear protein 1	3.5	5.7	5.3
Herpud1	homocysteine-inducible, endoplasmic reticulum stress-inducible, ub-like domain member 1	3.5	3.7	7.5
Mt2	metallothionein 2	1.4	1.6	1.5
Gtpbp2	GTP binding protein 2	1.7	1.9	3
1810045K07Rik	RIKEN cDNA 1810045K07 gene	1.4	1.7	2.6
Gclm	glutamate-cysteine ligase , modifier subunit	1.7	2.5	2.1
Jund1	Jun proto-oncogene related gene d1	1.4	1.7	1.6
Rnu22	RNA, U22 small nucleolar	2.8	3.5	4
Atf4	activating transcription factor 4	1.7	2.3	2.1
Ier3	immediate early response 3	1.7	1.7	2.5
Cars	cysteinyl-tRNA synthetase	2	2.1	2.5
Csrp1	cysteine and glycine-rich protein 1	1.7	2	2.3
Psph	phosphoserine phosphatase	1.6	1.7	2
Slc7a5	solute carrier family 7 (cationic amino acid transporter, y+ system), member 5	1.5	1.5	1.5
Ddr2	discoidin domain receptor family, member 2	1.5	1.6	1.4
Mthfd2	methylenetetrahydrofolate dehydrogenase (NAD+ dependent)	1.4	1.5	1.4
Dusp1	dual specificity phosphatase 1	2.5	2.8	2.6
Csrp1	cysteine and glycine-rich protein 1	1.6	2.1	2.1

Holtz

Gene	Description			
1500005G05Rik	RIKEN cDNA 1500005G05 gene	2.1	2.6	4
Aars	alanyl-tRNA synthetase	1.7	1.9	1.9
Slc3a2	solute carrier family 3 (activators of dibasic and neutral amino acid transport), member 2	1.7	2.1	2.5
5730493B19Rik	RIKEN cDNA 5730493B19Rik	1.4	1.9	1.7
Gas5	growth arrest specific 5	1.4	1.7	2.5
Sui1-rs1	suppressor of initiator codon mutations, related sequence 1 (S. cerevisiae)	1.4	1.5	1.5
Lars	leucyl-tRNA synthetase	1.5	2.1	2
Gdf15	growth differentiation factor 15	5.5	7.5	5.3

E430001P04Rik	RIKEN cDNA E430001P04 gene	1.4	1.4	1.5
Slc6a9	solute carrier family 6 (neurotransmitter transporter, glycine), member 9	1.9	2	1.4
Tars	threonyl-tRNA synthetase	1.4	1.9	2
Atf3	activating transcription factor 3	8.6	7.5	9.8
Nfe2l1	nuclear factor, erythroid derived 2,-like 1	2	1.6	1.5
3110065C23Rik	RIKEN cDNA 3110065C23 gene	1.7	1.7	1.9
Eif4ebp1	eukaryotic translation initiation factor 4E binding protein 1	1.9	2	1.9
Ifld2	induced in fatty liver dystrophy 2	5.7	6.1	3.7
Cebpb	CCAAT/enhancer binding protein (C/EBP), beta	3.2	3.7	5.3
D0Jmb3	DNA segment, Jeremy M. Boss 3	1.6	1.6	1.7
Arhb	ras homolog gene family, member B	1.9	2	2
Slc1a4	solute carrier family 1 (glutamate/neutral amino acid transporter), member 4	1.6	1.7	1.9
Nars	asparaginyl-tRNA synthetase	1.5	1.4	1.7
Ddit4	DNA-damage inducible transcript 4	2.1	1.5	1.9

A

3hr 6-OHDA induction (log.)

B

6hr 6-OHDA induction (log.)

C
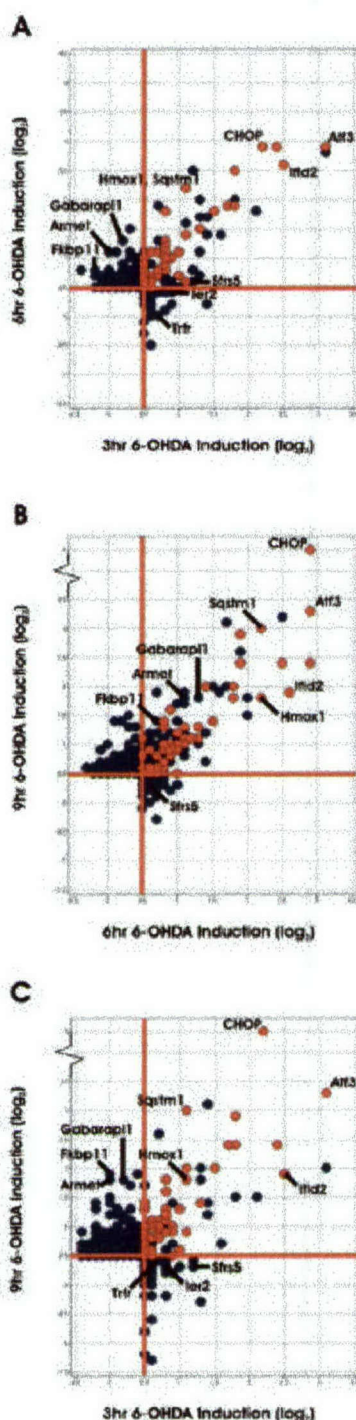

3hr 6-OHDA induction (log.)

Figure 1. Kinetic profiling reveals differential gene induction in response to toxin treatment.

One way to visualize these temporally complex changes is to plot the induction of genes increasing at one time point versus those increasing at another (Figure 1).

Red horizontal and vertical lines demarcate the threshold set for increasing transcripts (0.5 signal $\log_2$ ratio, ~1.5-fold change). Genes that fall to the right of the vertical red line were increased after 3 hours; those falling above the horizontal red line were increased after 6 hours (Figure 1A). Genes in the upper right quadrant were increased at both 3 and 6 hours (Figure 1A). Similarly, data were plotted for genes increasing at 6 versus 9 hours and genes increasing at 3 versus 9 hours, respectively (Figure 1B, 1C). Transcripts increased at all three time points are represented by red closed circles (Figure 1). In accordance with previous results, these include genes involved in cellular stress responses, signaling, transport, and the ubiquitin-proteasome pathway (Table 1). Similarly, these new data sets confirm and extend our prior findings showing that the stress-induced transcription factor CHOP (Ddit3/Gadd153) is dramatically upregulated at all time points (Figure 1, Table 1). Besides CHOP, the genes Atf3, Ifld2, Hmox1, and Sqstm1 are also robustly increased at all three times whereas Gabarapl1, Armet, and Fkpb11 are increased only at 6 and 9 hours (Figure 1, Table 1).

Another way to compare genes is by their individual signal levels at each time point as opposed to the ratio of their signal levels compared to control. Here signal values are first normalized across experiments via z-scores to make them directly comparable. The subsequent normalized values are used to generate an expression profile for each gene. Data mining software not only allows these expression profiles to be searched for other genes with similar kinetic patterns but also clusters genes together according to their profiles. Genes identified in Table 1 as increasing at all three time points are ranked according to the correlation of their expression profile with that of CHOP (Gadd153/Ddit3). Therefore, Hmox1 and Sqstm1 have expression profiles closest to CHOP whereas Slc1a4, Nars, and Ddit4 are the most dissimilar. It should be noted that signal level ranking does not necessarily correlate to fold inductions.
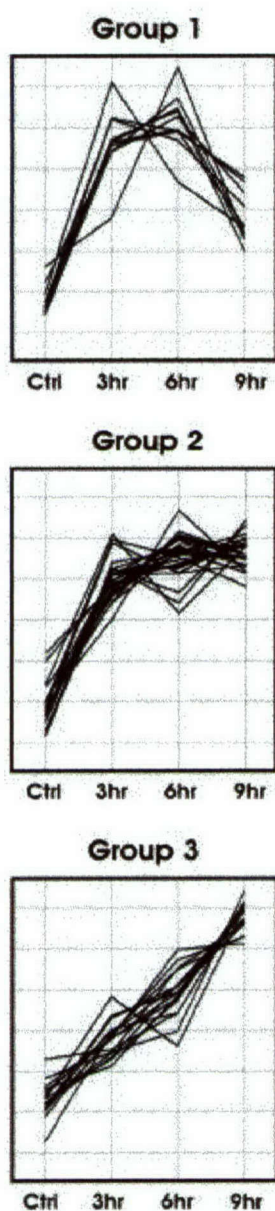
Group 1

Analysis of all genes noted in Table 1 (transcripts increased at all time points) using the k-means clustering algorithm generated three distinct kinetic profiles (Figure 2).

The first, Group 1, are early genes that increase in expression quickly, peaking between 3 and 6 hours. Group 2 genes also increase early but maintain their level of expression, whereas Group 3 genes are generally increasing throughout the time period measured. Overall, almost all of the gene profiles could be clustered into one of the three subgroups shown in Figure 2.

C. Verification in MN9D Cells

Group 2

Real Time PCR and Expression Profile Comparison: To verify the kinetic profiles and subgroupings identified on the basis of microarray data, we performed real time PCR analysis on selected genes. Figure 3 compares data generated from real time PCR experiments (circles and solid lines) with the expression profile generated from the normalized signal values of the microarray (squares and dashed lines).

Group 3

Figure 2. K-means clustering of increasing genes reveals three distinct expression profiles.
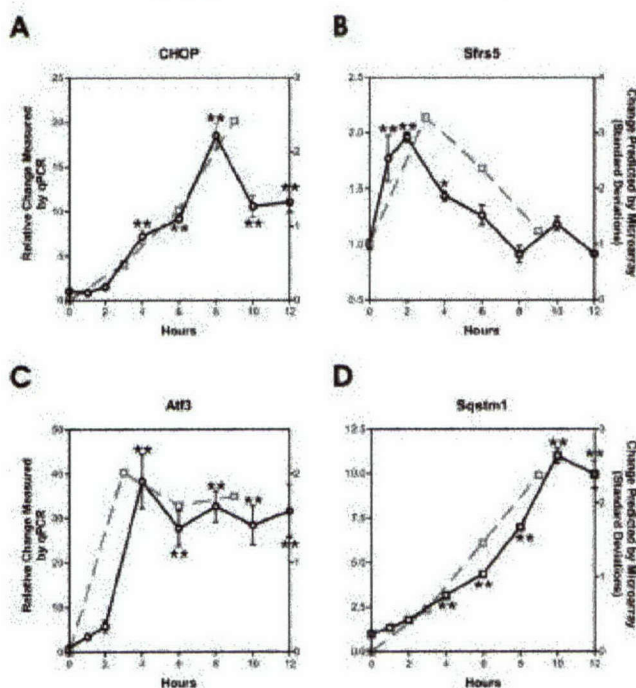
Figure 3. Real time PCR confirms microarray expression profiling. Total RNA was isolated from 6-OHDA-treated MN9D cells and used for reverse transcription PCR and real time PCR analysis using appropriate primers. Real time PCR results (circles and solid lines) correspond with their microarray profiles. Values represent mean ± S.E. of three to six replicate real time PCR reactions. **, $p < 0.01$ compared to untreated control.

The stress-induced transcription factor CHOP has previously been shown to be upregulated by 6-OHDA (Holtz and O'Malley, 2003). K-means cluster analysis placed CHOP in Group 3 of more slowly rising late genes described above. Figure 3A shows that the microarray profile generated

at 3, 6, and 9 hours is virtually identical to real time PCR measurements up to 8 hours. Because the microarray results do not extend beyond 9 hours, they do not predict the decrease observed by real time PCR at 10 and 12 hours. Microarray analysis indicates that splicing factor, serine/arginine rich 5 (Sfrs5) has a kinetic profile of a gene in Group 1, genes that peak quickly and then decrease. This early peaking profile was confirmed by real time PCR results (Figure 3B). Activating transcription factor 3 (Atf3) was placed by cluster analysis of the microarray data into the group of genes that increased rapidly and remained elevated (Group 2). Real time PCR corroborates this kinetic profile (Figure 3C). The gene sequestosome 1 (Sqstm1/p62) was clustered into the same group of late genes as CHOP, since the expression profiles of the two genes were highly correlated (Table 1). This similarity in expression profiles was confirmed by real time PCR (compare Figure 3D to 3A). PCR time points after 9 hours, however, reveal that Sqstm1 continues to increase after CHOP levels begin to fall. Taken together, the present microarray results were excellent predictors of bone fide transcript responses following toxin treatment. Of the genes identified as increasing at all three microarray time points, Hmox1 has an expression profile most closely correlated with CHOP. The Hmox-1 kinetic profile was verified via real time PCR analysis as well as Western blotting of cell lysates from 6-OHDA-treated MN9D cells (Figure 4). Both RNA and protein patterns indicate that Hmox1 expression parallels that of CHOP.
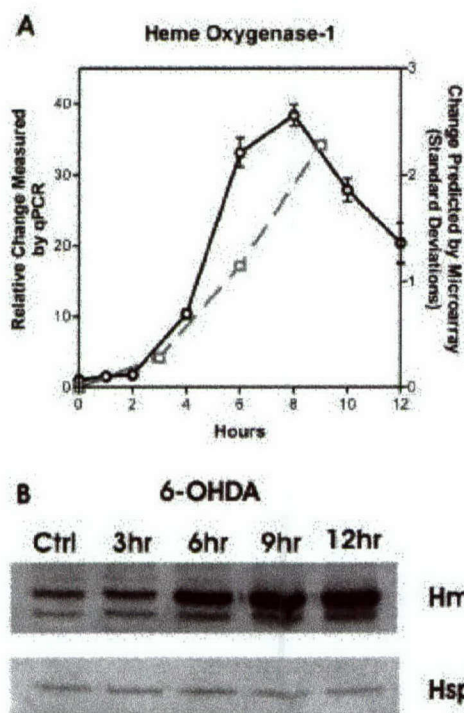

2D Gel Electrophoresis: With the advent of proteomics it is possible to examine the consequences of toxin treatment in complex cellular systems. Thus, MN9D cells were treated for six hours with 6-OHDA alone, 6-OHDA together with the anti-oxidant NAC, or MPP$^+$ alone. Two-dimensional electrophoresis was used to evaluate alterations in the levels of proteins following toxin exposure. Twenty-four proteins showed differential expression, twelve increased and twelve decreased, as a consequence of 6-OHDA treatment (Figure 5).

Figure 4. 6-OHDA induction of Heme Oxygenase-1 can be detected at the mRNA (A) and protein expression levels (B).
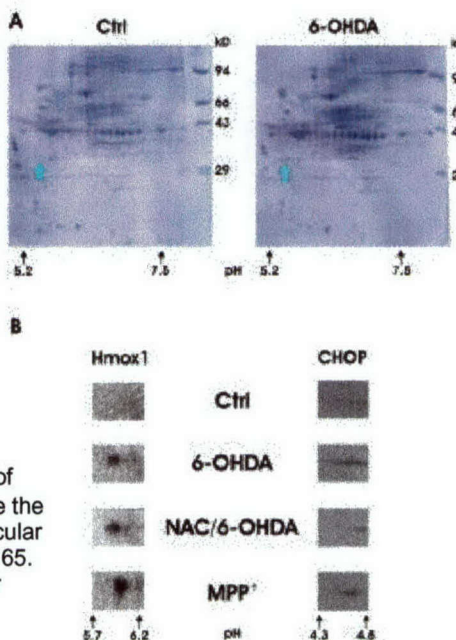
Figure 5. 2D gel electrophoresis identifies upregulation of CHOP and Hmox1 protein levels. A, Arrowheads denote the position of Hmox1 with a theoretical pI of 6.08 and molecular weight of 32 kDa. Mouse CHOP has a calculated pI of 4.65. (B) Proteins were transferred onto PDVF membranes for immunoblot detection with anti-Hmox1 or anti-CHOP antibodies.

10

The majority of these changes were blocked by pre-treatment with the antioxidant, NAC (not shown). Of these proteins, CHOP and Hmox1 were further examined by Western blotting. Both proteins were barely detectable in untreated control samples, and both were robustly upregulated in either 6-OHDA- or MPP$^+$- treated cells. Surprisingly only CHOP activation was blocked by NAC pre-treatment. Hmox1 was less affected (Figure 5B). Taken together, these data confirm and extend results derived from global genome analysis to the level of the proteome. These reports are in press in the journal Antioxidants and Free Radicals.

6-OHDA Signaling Pathways: In separate studies we have previously shown that 6-OHDA rapidly induces ROS (Lotharius et al., 1999) as well as triggering ER stress and the UPR in primary dopaminergic neurons (Holtz and O'Malley, 2003). To test the hypothesis that ROS generation is upstream of 6-OHDA-mediated UPR, we utilized a variety of reagents and techniques to determine the nature and the timing of 6-OHDA-generated free radicals in MN9D cells. For example, ROS production in situ was determined using the cell permeable indicator DCF together with real-time confocal imaging of single cells following 6-OHDA addition (Figure 6).

Figure 6. 6-OHDA rapidly induces ROS monitored in real time by measuring increased fluorescence of DCF via confocal microscopy.

Application of 6-OHDA led to rapid changes in DCF fluorescent intensity that plateaued in about 2-3 minutes. As DCF detects various oxidizing species including superoxide anion, hydrogen peroxide, and nitric oxide, any or all of these types of radicals might be present. This early increase in oxidative species precedes the appearance of markers of UPR and/or apoptosis that have been observed following 6-OHDA mediated cell death (Holtz and O'Malley, 2003).

To confirm that 6-OHDA induces ROS formation in a time frame preceding the appearance of UPR markers, NAC was used to order and block 6-OHDA toxicity. Consistent with our previous results demonstrating that antioxidants save 6-OHDA-mediated cell death in primary dopamine neurons (Lotharius et al., 1999), 5 mM NAC completely blocked up to 100 µM 6-OHDA-induced death of MN9D cells (Figure 7A).

Moreover, 6-OHDA-induced ROS is necessary for 6-OHDA-induced UPR since pretreatment with NAC robustly blocked up-regulation of multiple stress-induced genes including phosphorylation of eIF2a and increased ATF3 at 3 and 6 hours (Figure 7B). NAC also blocked phosphorylation of c-jun and SAPK/JNK, as well as increases in CHOP and HO-1 levels at 9 and 12 hours (Figure 7C). In addition, NAC blocked the downstream activation of caspase-3 and caspase-9 (Figure 7C).

Figure 7. The antioxidant NAC is able to block 6-OHDA-induced cell death (A) as well as markers of UPR and apoptosis (B,C).
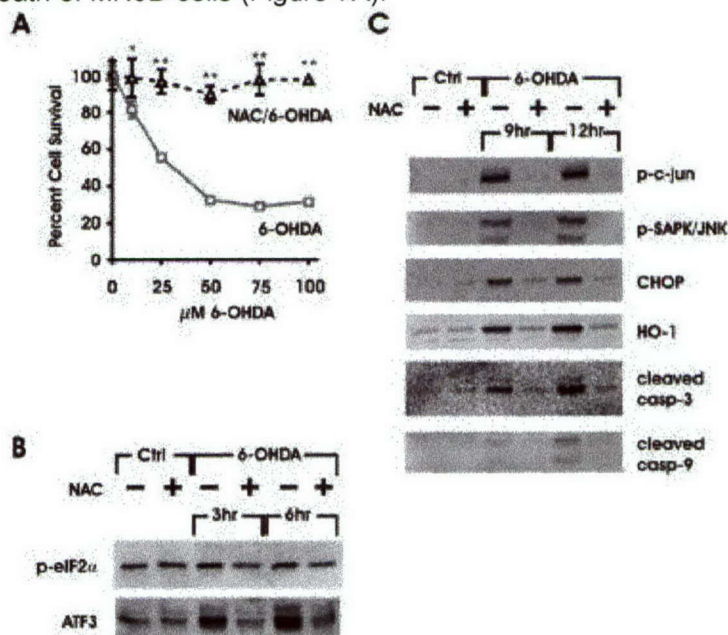
Thus, 6-OHDA induces coordinated up-regulation of UPR genes through the generation of oxidative stress.

Mitochondrial events are downstream of UPR up-regulation: An important question is whether the intrinsic mitochondrial apoptotic pathway plays a parallel or sequential role to UPR in 6-OHDA mediated cell death. Because cytochrome c release from the mitochondria precedes caspase activation (Danial and Korsmeyer, 2004), the timing of its release in relation to UPR activation was used to determine the role of the mitochondrial pathway. Subcellular fractionation of 4, 8, and 16 hour 6-OHDA-treated cells along with vehicle or NAC-treated controls revealed that changes in cytochrome c distribution are not apparent until 8-16 hours post drug treatment (Figure 8), well after UPR upregulation (Figure 7B). Release of cytochrome c is robustly blocked by NAC. Consistent with our earlier studies (O'Malley et al., 2003), Bax was not translocated from cytoplasmic to mitochondrial compartments over the time course of this experiment (Figure 8). These data, together with the finding that activation of caspase-3 and -9 is a late event occurring 8-12 hours after 6-OHDA addition (Figure 7C), suggests that mitochondrial changes occur subsequent to UPR associated events.
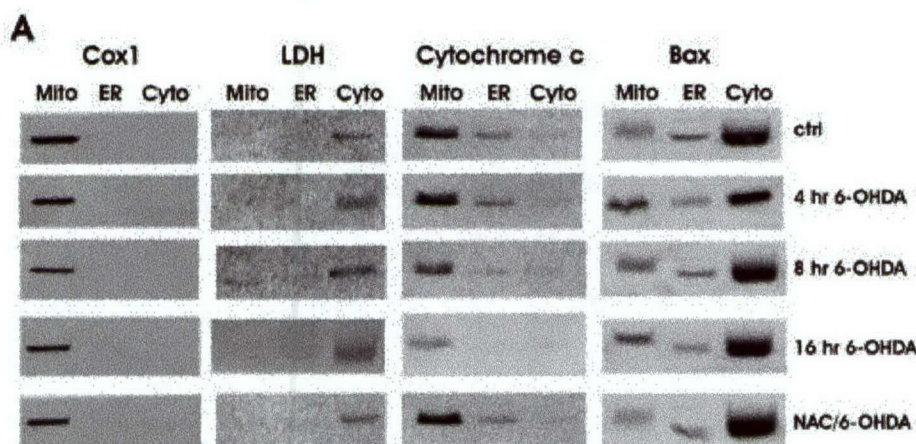
A

Figure 8. Mitochondrial release of cytochrome c is downstream of 6-OHDA-induced UPR. Subcellular fractionation of MN9D cells was performed to obtain mitochondrial (mito), ER, and cytoplasmic (cyto) fractions from cells treated for 4, 8, or 16 hours with 75 µM 6-OHDA. Cells were also co-treated with 6-OHDA and 5 mM NAC for 16 hours. Fractions were Western blotted with anti- COX1 and anti-LDH confirming compartmental designations as well as anti-cytochrome c and Bax to detect changes in localization.
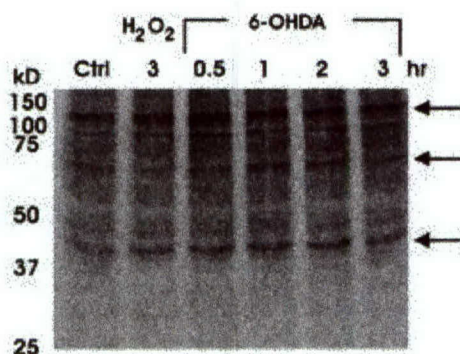
**6-OHDA causes oxidative modification of proteins**: Unchecked generation of ROS can result in oxidative damage to macromolecules including proteins, lipids, and DNA (Jenner, 2003). Oxidative protein modification can impair proper protein degradation and lead to UPR up-regulation. Because strong activation of early UPR markers such as phosphorylation of SAPK/JNK and increased ATF3 are evident after only 3 hours of 6-OHDA treatment (not shown), oxidative modification of proteins would have to occur rapidly to be the trigger of coordinated stress gene response. Indeed, after only 30 minutes of exposure to 6-OHDA, carbonyl modification of proteins is detected in MN9D lysates (Figure 9).

Figure 9. 6-OHDA causes the rapid oxidative modification of proteins. Carbonyl groups generated by oxidative stress were subjected to DNPH-derivitization and increases in oxidatively modified proteins were detected with an antibody against DNP.

12

Four distinct bands of molecular weights of 40, 70, and 120 kD were identified as specific ROS targets. These results are consistent with a model by which 6-OHDA rapidly induces ROS generation, leading to oxidative protein modification, which in turns impairs protein degradation and triggers cellular stress.

6-OHDA induces an increase in polyubiquitinated proteins: Polyubiquitination of proteins serves as a mechanism to mark un-needed or damaged proteins for degradation (Sherman and Goldberg, 2001). 6-OHDA exposure to MN9D cells increased polyubiquitinated proteins in a time-dependent manner (Figure 10A, B).
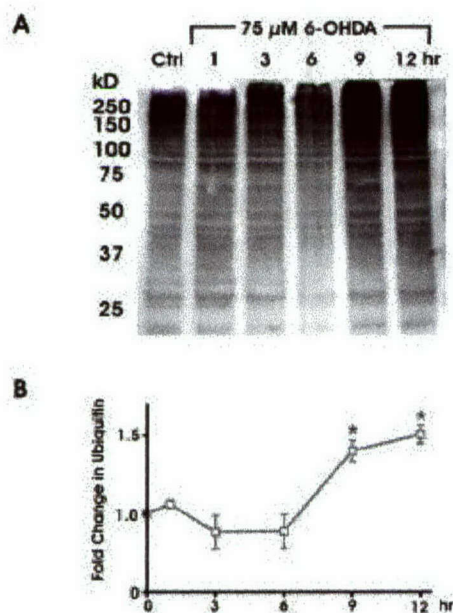

Quantification of band intensity across multiple experiments indicates a 1.5 fold increase in polyubiquitinated proteins at 9 and 12 hours. This increase is significantly different from early time points, suggesting the accumulation of oxidatively damaged proteins that have been marked for disposal.

D. Are neurotoxin-mediated changes in gene expression recapitulated in cultured dopaminergic neurons?

To confirm and extend results obtained using the dopaminergic cell line model, we are using primary cultures of dopaminergic neurons. The advantages of using this paradigm include the ease of preparation and culture manipulation and the well-documented similarity in responses (Oh et al., 1995; Lotharius et al., 1999; Holtz and O'Malley, 2003). In the last report we showed that 6-OHDA increased levels of CHOP protein at 6 and 12 hours. 6-OHDA also increased phosphorylation of

Figure 10. 6-OHDA causes a late increase in levels of polyubiquitinated proteins. (A) Protein lysates were isolated from MN9D cells and subjected to Western blot analysis using an antibody that detects polyubiquitinated proteins. (B) Quantification of polyubiquitinated proteins was performed by quantitative fluoroimaging. Values represent the mean ± SEM of triplicate Western blots. *P < 0.05 compared to untreated control.
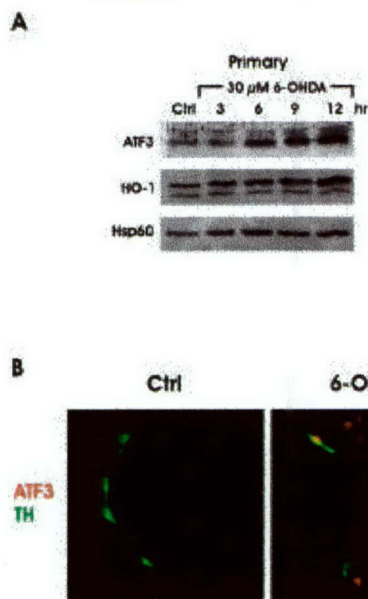
eIF2α and c-jun. Further evidence of cell stress/UPR is apparent by the induction of ATF3 in lysates from primary dopaminergic cultures (Figure 11A) as well as in nuclei of dopamine synthesizing neurons (Figure 11B).

Figure 11. 6-OHDA induces markers of cellular stress in primary dopaminergic cultures. Treatment with 6-OHDA increased (A) levels of ATF3 and HO-1 protein in lysates isolated from primary dopaminergic cultures as detected by Western blot analysis. (B) Primary cultures were fixed after 4 hours of 6-OHDA treatment and co-stained with antibodies against ATF3 and TH. Left panel shows no to low ATF3 staining in control cultures. Distinct nuclear localization of ATF3 following 6-OHDA can be observed in the right panel including within TH positive neurons.

Our previous findings demonstrated that antioxidants such as fullerenes completely protected primary dopaminergic cells from cell death (Lotharius et al., 1999). Immunostaining similarly treated cultures revealed that NAC antioxidant treatment blocked 6-OHDA-mediated nuclear CHOP accumulation as well as caspase-3 activation (Figure 12A).
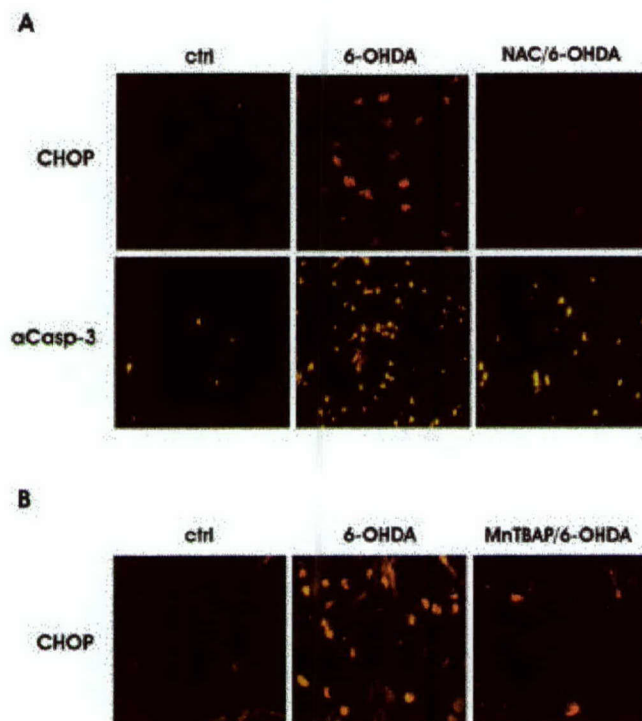
The superoxide dismutase mimetic MnTBAP has also been shown to be protective against 6-OHDA (Choi et al., 2004). Pretreatment of primary midbrain cultures with MnTBAP also prevents CHOP up-regulation (Figure 12B). These results not only demonstrate the similarity between MN9D cells and primary dopaminergic neurons, but also show that the prevention of 6-OHDA-induced UPR via ROS attenuation is not unique to NAC.

Figure 12. Antioxidants, NAC (A) or MnTBAP (B), block 6-OHDA-induced markers of UPR in primary dopaminergic cultures.

Key Research Accomplishments

Analyzed hybridization patterns of normal and 9-hour toxin-treated cRNAs using in-house GeneChip Facility and Affymetrix 12,000 gene chip set.

Established real time PCR techniques to evaluate microarray data.

Verified differential regulation of particular gene subsets using RNA, Western blot, and immunocytochemical analysis in MN9D cells and cultured dopaminergic neurons.

Discovered that both MPP$^+$ and 6-OHDA induce markers of ER stress.

Determined that 6-OHDA induces the upregulation of ER stress/UPR via generation of ROS.

Delineated many signaling pathways mediating neurotoxin responses.

Established time course of events underlying 6-OHDA toxicity.

Reportable Outcomes

A poster describing our initial studies was presented at the Society for Neuroscience Annual Meeting, 2002.

A slide presentation describing our then current studies was presented at the Society for Neuroscience Annual Meeting, 2003.

A poster describing our ongoing studies will be presented at the Society for Neuroscience Annual Meeting, 2004.

Papers and manuscripts:

Holtz WA and O'Malley KL (2003) Parkinsonian mimetics induce aspects of unfolded protein response in death of dopaminergic neurons. J Biol Chem. 278:19367-77. Epub 2003 Feb 21.

Holtz WA, Turetzky, JM and O'Malley KL (2004) Microarray expression profiling identifies early signaling transcripts associated with 6-OHDA-induced dopaminergic cell death. Antioxidants and Redox Signalling, in press.

Holtz WA, Turetzky, JM and O'Malley KL (2004) Oxidative stress-triggered unfolded protein response is upstream of intrinsic cell death evoked by parkinsonian mimetics. J. Neuroscience, submitted.

Conclusions

The central hypothesis of these studies is that changes in gene expression underlie much of the damage that ultimately leads to the death of dopaminergic neurons after treatment with 6-OHDA or MPP$^+$. Using DNA microarray technology we determined that both of these neurotoxins primarily induce ER stress although not to the same degree. Subsequent efforts to identify key genetic components of this response have suggested new points of intervention. Taken together, these experiments will help clarify the molecular mechanisms associated with 6-OHDA and MPP$^+$ toxicity and might aid in developing novel therapeutic avenues to pursue relevant to PD.

6-OHDA and MPP$^+$ induce ER Stress/UPR

Our initial study reported in 2003 (Holtz and O'Malley) utilized gene expression profiling to assess thousands of genes in order to obtain a more detailed understanding of the molecular programs utilized by dopaminergic cells in response to 6-OHDA and MPP$^+$. Two important outcomes from this study include the identification of a previously unsuspected link between these known oxidative stress inducers and aspects of ER stress/UPR, as well as the identification of at least a subset of common transcriptional changes associated with toxin-mediated events. The latter observation emphasizes the overlapping yet divergent nature of cell death in response to 6-OHDA versus MPP$^+$.

Commonality in response to 6-OHDA and MPP$^+$ is highlighted by the finding that the most highly induced transcript by either toxin was CHOP, a stress-induced transcription factor implicated in cell death. The temporal and spatial up-regulation of CHOP was confirmed and extended by RT-PCR, Western blot analysis, and immunocytochemistry. In support of the present findings,

microarray analysis of MPP$^+$ treated SH-SY5Y cells also resulted in an up-regulation of CHOP, albeit with a much later, more prolonged time course (Conn et al., 2002). Similarly, microarray analysis of the dopaminergic cell line, SN4741, revealed induction of stress indices following MPP$^+$ treatment (Chun et al., 2001). To date however, this was the first report that 6-OHDA up-regulates CHOP, and that it does so to a much greater extent than MPP$^+$.

Additional transcripts identified via microarray analysis revealed that 6-OHDA induced a large number of genes that were not positively affected by MPP$^+$, many of which were involved in protein folding, trafficking, or degradation. In contrast, the subset of genes induced by both drugs included amino acid transporters, tRNA-synthetases, ion channels, and stress induced transcription factors. A small number of genes was induced by MPP$^+$ but not 6-OHDA. These included Dnaja3, adaptor-related protein complex AP-3 beta 1 subunit, and mylin transcription factor 1. Currently, the significance of these changes is unclear. Overall, MPP$^+$ induced transcripts appeared to primarily represent a subset of genes induced by 6-OHDA.

UPR signaling pathways: Three signaling pathways have been associated with UPR that are triggered by the ER proteins, Ire1a/ß, ATF6 and PERK (Ma and Hendershot, 2001). The Ire1a/ß pathway is thought to activate caspase-12, the JNK/SAPK pathway, as well as Xbp1 mRNA splicing. Translocation of ATF6 to the nucleus leads to the up-regulation of Xbp1 as well as various ER chaperones. Finally, in addition to transcriptional changes, ER stress/UPR can down-regulate protein translation through phosphorylation of eIF2α via PERK kinase activity. GeneChip analysis indicated that many of the genes induced by either MPP$^+$ or 6-OHDA were increased to a similar extent. A notable exception, however, was that 6-OHDA induced CHOP 26-fold compared to 9-fold with MPP$^+$ (Holtz and O'Malley, 2003). Moreover, although both neurotoxins increased ATF4 and C/EBPß, only 6-OHDA increased Xbp-1 mRNA levels. These data are consistent with the notion that 6-OHDA triggered both ATF6 and PERK pathways leading to the dual activation of the CHOP promoter. Moreover, processing of Xbp1 mRNA and increased phospho-c-jun levels indicating activation of the Ire1α/β pathway, was only observed with 6-OHDA. These data led us to propose that 6-OHDA is activating all three branches of the UPR signaling cascade, Ire1a/ß, ATF6 and PERK whereas MPP$^+$ is only activating the PERK branch.

6-OHDA- or MPP$^+$-mediated cell death: Previously we and others have shown that although 6-OHDA and MPP$^+$ both generate oxidative stress, only 6-OHDA treatment resulted in activation of caspases and morphological changes associated with apoptosis (Lotharius et al., 1999). Several lines of evidence from this laboratory suggest, however, that 6-OHDA does not mediate an intrinsic, mitochondrial-dependent, apoptotic pathway. For example, overexpression of the anti-apoptotic protein, Bcl-2, did not attenuate 6-OHDA induced cell death in either the MN9D cell line or in primary dopaminergic neurons (O'Malley et al., 2003). Moreover, deletion of the pro-apoptotic Bcl-2 family member, Bax, did not rescue dopamine neurons from 6-OHDA toxicity (O'Malley et al., 2003), nor was Bax protein translocated to the mitochondria in response to this toxin (Holtz et al., 2004b). Finally, microarray analysis failed to detect up-regulation of any BH3-only family proteins thought to act upstream of the intrinsic mitochondrial pathway, even though downstream caspases were activated (Holtz and O'Malley, 2003). Thus, these data support a model in which 6-OHDA activates apoptosis via non-canonical pathways.

Following transient increases, MPP$^+$-induced phospho-PERK, phospho-eIF2α, and phospho-c-jun levels all decreased to near control levels after 6 to 9 hours of exposure, whereas these same proteins remained phosphorylated in response to 6-OHDA (Holtz and O'Malley, 2003). Why then are MPP$^+$ mediated changes transient? One possible explanation is that although both toxins initially trigger the same response due to oxidative stress, this response diverges as

MPP$^+$ more effectively depletes cellular energy. Conceivably only 6-OHDA-treated cells retain sufficient energy to execute apoptosis. On the other hand, BiP and Xbp1 mRNA did not increase significantly at any time following MPP$^+$ treatment, but were induced by 6-OHDA. This might indicate that the two responses are distinct from the beginning, despite sharing common participants.

In primary cultures, the difference between 6-OHDA and MPP$^+$ appears to be even more distinct. Markers of UPR seen in 6-OHDA treated MN9D cells were also seen in 6-OHDA treated primary cultures (Holtz and O'Malley, 2003). In contrast, MPP$^+$ did not appear to up-regulate CHOP or to phosphorylate eIF2a or c-jun in dissociated dopaminergic neurons. Further investigation will be needed to determine if this is due to differences between MN9D cells and primary cells, or due to the manner or timing in which the cells were treated.

Microarray expression profiling identifies early signaling transcripts associated with 6-OHDA-induced dopaminergic cell death

 Building on the previous report showing that cellular stress plays a role in PD (Holtz and O'Malley, 2003), a subsequent study identified complex temporal changes associated with aberrant protein degradation following neurotoxin treatment. By analyzing microarray data, distinct functional subgroups of genes were revealed. Notably, stress-induced transcription factors such as ATF3, ATF4, CHOP, and C/EBPß were all robustly induced yet exhibited unique kinetic patterns. Multi-faceted expression profiles were also observed for genes involved in the synthesis and modification of proteins (e.g. six different tRNA synthetases), protein degradation (e.g. ubiquitin, Herpud1, Sqstm1), oxidative stress (Hmox1, Por), etc. Taken together these data support the notion that oxidative stress and protein dysfunction play a role in PD as well as provide a time course for many of the molecular events associated with 6-OHDA neurotoxicity (Holtz et al., 2004b).

Clustering of genes involved in 6-OHDA-induced cell death: The ability to group genes based on temporal expression patterns is an important means by which functional relationships or common regulatory mechanisms can be identified. Despite the very large data sets generated from microarray experiments, continually updated algorithms and software can be utilized to filter raw information into smaller collections of significance as well as to cluster transcripts into distinct kinetic profiles. To identify sets of genes of interest, we first filtered genes to single out those that were increasing at each time point. Subsequent comparison of genes induced at one time point against those induced at a different time revealed genes that were distinct to those times as well as genes that were increased at multiple times. Genes could be further ranked according to their correlation to a particular gene or profile. Because of its large induction, and response to a broad range of insults, we initially focused on the transcription factor CHOP. Genes were ranked according to their kinetic similarity to that of CHOP, which was used as an "anchor". This approach allows for identification of those genes that potentially share functional properties or regulatory elements. By using other genes of interest as anchors, and searching larger data sets for similar expression profiles, de novo associations may be discovered.

Application of K-means clustering revealed additional relationships based on shared kinetic pattern profiles including Group 1 (rapid rise and decline), Group 2 (rapid rise with plateau) and Group 3 (late rise). Conceivably, expression of genes in Groups 1 and 2 may be closely linked to mechanisms that sense cellular changes and thus be required to initiate downstream

responses. In contrast, genes in the third group may be involved in either the cell's adaptive response to stress or in the execution of a cell death program.

Identification of genes involved in 6-OHDA-induced cell death: The Arg-Ser-rich domain protein, Sfrs5, is a member of a conserved family of splicing factors that can regulate alternative splicing (Du et al., 1998). Sfrs5 was identified as an immediate early gene in insulin-treated rat hepatoma H35 cells (Diamond et al., 1993), and identified as a Group 1, rapidly rising then declining gene, in the current study (Figure 3B). Several examples exist of alternate mRNA splicing being utilized as a mechanism for regulating stress response. During the unfolded protein response, the ER stress sensing protein, Ire1, mediates the unconventional splicing of Xbp1 mRNA to generate an active transcription factor (Lee et al., 2002). This splicing event has previously been confirmed following 6-OHDA-treatment (Holtz and O'Malley, 2003). In addition, the stress-induced transcription factor ATF3 (see below) also undergoes stress-induced alternative mRNA splicing to generate truncated isoforms that may modulate the activity of the full-length protein (Pan et al., 2003). Although Sfrs5 has not been directly implicated in alternative ATF3 splicing, the early profile of this transcript is consistent with a role in regulating downstream events.

Along with CHOP, the transcription factor ATF3 is one of the most highly induced genes (Table 1). Studies have shown that ATF3 is an integral part of the stress cascade, increasing in response to activation of the eIF2 kinases PERK or GCN2, which sense endoplasmic reticulum stress or amino acid starvation, respectively (Jiang et al., 2004). Induction of ATF3 depends upon the related bZIP transcription factor ATF4, which was also induced by 6-OHDA exposure. Enhanced levels of ATF4 are achieved via increased transcription as well as by selective mRNA translation despite the general attenuation of this process (Harding et al., 2003). Unlike CHOP, whose timing suggests a more downstream role in stress response (compare Figure 3A to 3C), early induction of ATF3 is consistent with a more immediate function in the coordination of stress induced gene expression.

Sqstm1 (p62), a gene encoding a ubiquitin (Ub)-binding protein, has been shown to be upregulated during apoptosis and proteasomal inhibition in neuronal cells (Kuusisto et al., 2001) as well as being localized to inclusion bodies in neurodegenerative disorders such as Alzheimer's and Parkinson's diseases (Zatloukal et al., 2002). In SH-SY5Y neuroblastoma and PC-12 cell lines, 6-OHDA has been shown to increase the levels of ubiquitin-conjugated proteins (Dawson and Mandir, 2002). Here, Sqstm1 expression was found to steadily rise over 10 hours following 6-OHDA treatment (Figure 3D). This pattern of expression is consistent with Sqstm1 playing a role in the aggregation of accumulating ubiquitinated proteins.

The late expression profile of Hmox1 was similar to Sqstm1 (compare Figure 3D to 4A). Hmox1 has been identified as a component of Lewy body inclusions in Parkinson's disease (Schipper et al., 1998), as well as being induced in response to a wide range of cellular stresses including oxidative insult of the nigral dopaminergic cell line SN4741 with hydrogen peroxide or MPP$^+$ (Salinas et al., 2003). Hmox1 functions as an important cellular antioxidant, and an increase in its expression protects against 6-OHDA in PC12 cells (Salinas et al., 2003). As with CHOP and Sqstm1, the timing of Hmox1 induction suggests a downstream role in the stress response, instead of a regulatory role.

Validation of Microarray expression profiling: Real time PCR analysis confirmed that microarray results were predicative of changes for selected genes (Figure 3). Further, Western blot analysis showed that the induction of the gene Hmox1 at the transcript level was consistent with induction of protein levels (Figure 4). Finally, proteomic analysis via 2-dimensional

electrophoresis also confirmed upregulation of Hmox1 as well as the previously identified 6-OHDA-induced stress marker CHOP (Figure 5). The latter approach has the power to resolve hundreds to thousands of proteins on a single gel. Caveats exist, however. For example, protein preparation using conventional techniques skews results towards hydrophilic proteins. Because cellular stress most likely involves membrane proteins from a variety of sources such as the ER, mitochondria and/or plasma membranes, alternate protein separation techniques may be required to assess complex protein changes following neurotoxin treatments. Present findings indicate that at least 24 proteins are changed in the narrow pI range between 5-8 due to 6-OHDA treatment (Figure 5 and not shown). Experiments including different pI ranges as well as native gels (Schèagger et al., 1998) will allow assessment of the complete proteome as well as protein:protein interactions. The latter may be particularly important in the cell's response to stress.

Review Response: The June 10th, 2004 Review by the American Institute of Biological Sciences noted that although significant progress had been made in completing the aims of this proposal that additional data acquisition and evaluation were necessary. In particular, they took us to task for not analyzing all of the toxin-altered transcripts or presenting data from additional time points. Finally, reviewers questioned our inability to detect changes in apoptotic pathways in response to these toxins and questioned our efforts in evaluating data acquired. It's worth noting here that our efforts at datamining were guided by experts in this field as well as by weekly input by the outstanding computational biology group here at Washington University School of Medicine. The latter would remind us that frequently microarray experiments do NOT reveal particular pathways, or show that so many genes are changing in response to the stimulus that it becomes extremely challenging to ascertain what the most significant response might be. The fact that an entirely unexpected pathway was discernable provided us with a framework that could subsequently be verified in vitro and in vivo. Finally, it's worth remembering, that transcriptional changes are just that: fluctuations in the level of a particular gene's expression. Real meaning in gene fluctuations comes from confirming changes at the level of the protein encoded for. Given our finding that the majority of genes induced more than two-fold in our system could all be firmly placed in the ER stress/UPR pathway (Holtz and O'Malley, 2003), we would have been remiss in not confirming via every available means that this was a bone fide response.

We entirely agree with reviewers that data acquired from additional time points was absolutely requisite in determining a full toxin-mediated response. In fact as mentioned in the last Progress Report, the additional samples were already prepared and were awaiting chip hybridization at the Washington University School of Medicine Microarray facility. With unlimited resources perhaps we could have obtained these data more rapidly. However, monies provided under the auspices of this award were predicated upon the significantly discounted costs available via our in-house shared facility. As such, users had to queue up. As indicated by the attached manuscripts/papers, we utilized our "waiting periods" to verify many aspects of the proposed model. Analysis of these data formed the core of our paper entitled "Microarray expression profiling identifies early signaling transcripts associated with 6-OHDA-induced dopaminergic cell death" by Holtz et al., (2004a). These results strengthened the original finding that ER stress/UPR was an early and robust response to toxin treatment.

Finally, as indicated above and extensively discussed in the last Progress report, there was very little evidence of canonical apoptotic changes at any time point. This is entirely in keeping with our previous results suggesting that BH3 proteins such as Bax, Bim, Bid, and Bak were not changing in terms of their overall transcription levels, their protein levels, or their phosphorylation status. These data are consistent with a model in which ER stress/UPR is

upstream of mitochondrial changes and proceeds without the aforementioned BH3 proteins (Holtz et al., 2004b). In contrast, a newly described BH3 protein, PUMA, does change. As an ER resident protein, PUMA may represent a link between ER stress and mitochondrial changes. PUMA was not on the microarray that we screened although it is on the latest chips.

Research Implications:

Unraveling the biological processes by which PD mimetics induce their neurotoxic effects is important to accurately model this disease. However, despite decades of use, the complex signaling pathways by which 6-OHDA and MPP$^+$ act remain unclear. The unsuspected finding that 6-OHDA and MPP$^+$ trigger components of the UPR pathway will lead to a better understanding of the application of these agents in models of nigral degeneration and improve the interpretation of the results. Moreover, our more recent findings can be used to construct a temporal model of events associated with 6-OHDA toxicity (Figure 13).
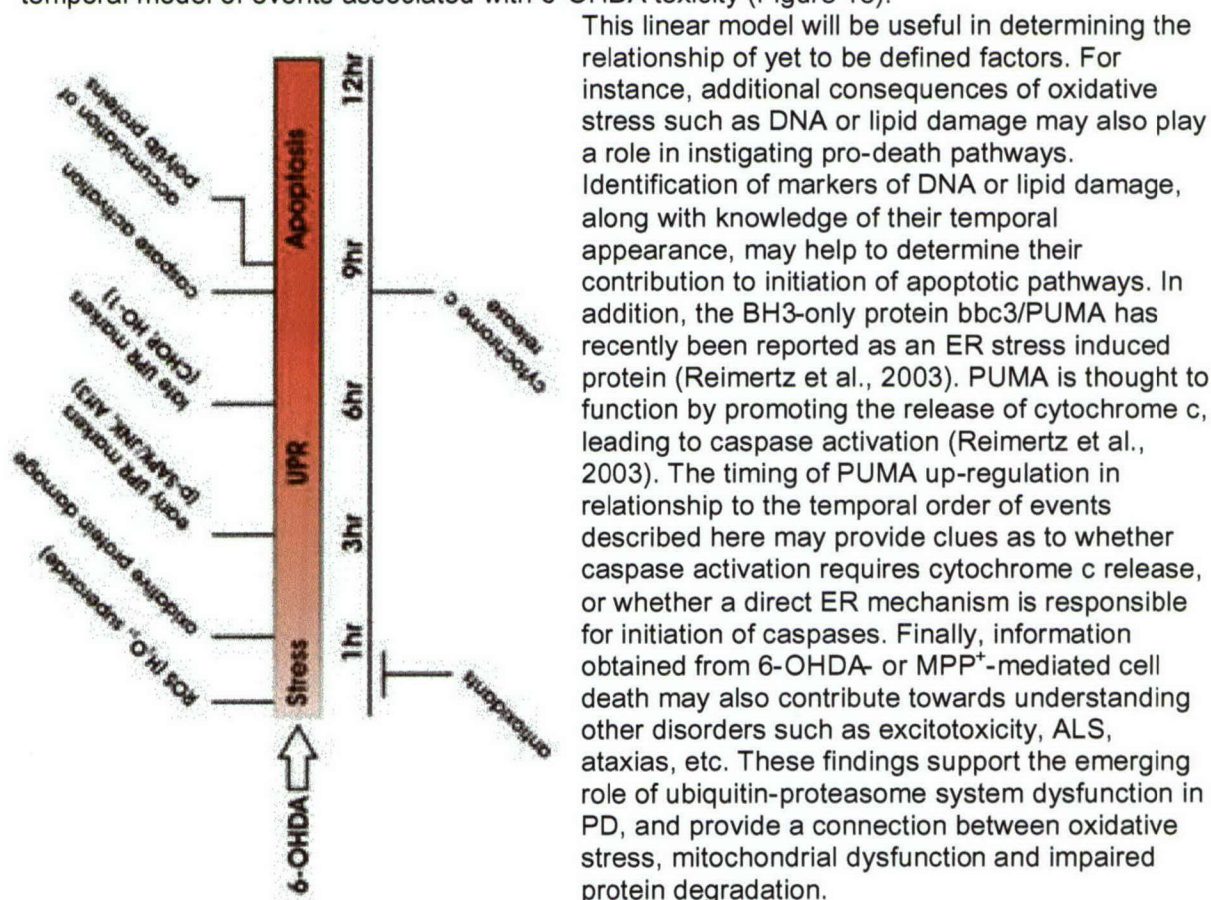

This linear model will be useful in determining the relationship of yet to be defined factors. For instance, additional consequences of oxidative stress such as DNA or lipid damage may also play a role in instigating pro-death pathways. Identification of markers of DNA or lipid damage, along with knowledge of their temporal appearance, may help to determine their contribution to initiation of apoptotic pathways. In addition, the BH3-only protein bbc3/PUMA has recently been reported as an ER stress induced protein (Reimertz et al., 2003). PUMA is thought to function by promoting the release of cytochrome c, leading to caspase activation (Reimertz et al., 2003). The timing of PUMA up-regulation in relationship to the temporal order of events described here may provide clues as to whether caspase activation requires cytochrome c release, or whether a direct ER mechanism is responsible for initiation of caspases. Finally, information obtained from 6-OHDA- or MPP$^+$-mediated cell death may also contribute towards understanding other disorders such as excitotoxicity, ALS, ataxias, etc. These findings support the emerging role of ubiquitin-proteasome system dysfunction in PD, and provide a connection between oxidative stress, mitochondrial dysfunction and impaired protein degradation.

Figure 13. Timeline of 6-OHDA-induced events.

References

Choi WS, Eom DS, Han BS, Kim WK, Han BH, Choi EJ, Oh TH, Markelonis GJ, Cho JW, Oh YJ. (2004) Phosphorylation of p38 MAPK induced by oxidative stress is linked to activation of both caspase-8- and -9-mediated apoptotic pathways in dopaminergic neurons. J Biol Chem 279:20451-60.

Chun HS, Gibson GE, DeGiorgio LA, Zhang H, Kidd VJ, Son JH. (2001) Dopaminergic cell death induced by MPP(+), oxidant and specific neurotoxicants shares the common molecular mechanism. *J Neurochem* 76:1010-1021.

Conn KJ, Gao WW, Ullman MD, McKeon-O'Malley C, Eisenhauer PB, Fine RE, Wells JM. (2002) Specific up-regulation of GADD153/CHOP in 1-methyl-4-phenyl-pyridinium-treated SH-SY5Y cells. J Neurosci Res. 68:755-60.

Danial NN, Korsmeyer SJ. (2004) Cell death: critical control points. Cell 116:205-19.

Dawson T, Mandir A, Lee M. (2002) Animal models of PD: pieces of the same puzzle? *Neuron* 35:219-222.

Diamond RH, Du K, Lee VM, Mohn KL, Haber BA, Tewari DS, Taub R. (1993) Novel delayed-early and highly insulin-induced growth response genes. Identification of HRS, a potential regulator of alternative pre-mRNA splicing. *J Biol Chem* 268:15185-15192.

Du K, Leu JI, Peng Y, Taub R. (1998) Transcriptional up-regulation of the delayed early gene HRS/SRp40 during liver regeneration. Interactions among YY1, GA-binding proteins, and mitogenic signals. *J Biol Chem* 273:35208-35215.

Harding HP, Zhang Y, Zeng H, Novoa I, Lu PD, Calfon M, Sadri N, Yun C, Popko B, Paules R, Stojdl DF, Bell JC, Hettmann T, Leiden JM, Ron D. (2003) An integrated stress response regulates amino acid metabolism and resistance to oxidative stress. *Mol Cell* 11:619-633.

Holtz WA, O'Malley KL. (2003) Parkinsonian mimetics induce aspects of unfolded protein response in death of dopaminergic neurons. J Biol Chem. 278:19367-77.

Holtz WA, Turetzky, JM and O'Malley KL (2004) Microarray expression profiling identifies early signaling transcripts associated with 6-OHDA-induced dopaminergic cell death. Antioxidants and Redox Signalling, in press.

Holtz WA, Turetzky, JM and O'Malley KL (2004) Oxidative stress-triggered unfolded protein response is upstream of intrinsic cell death evoked by parkinsonian mimetics. J. Neuroscience, submitted.

Jenner P. (2003) Oxidative stress in Parkinson's disease. Ann Neurol. 53 Suppl 3:S26-36.

Jiang HY, Wek SA, McGrath BC, Lu D, Hai T, Harding HP, Wang X, Ron D, Cavener DR, Wek RC. (2004) Activating transcription factor 3 is integral to the eukaryotic initiation factor 2 kinase stress response. *Mol Cell Biol* 24:1365-1377.

Kuusisto E, Suuronen T, Salminen A. (2001) Ubiquitin-binding protein p62 expression is induced during apoptosis and proteasomal inhibition in neuronal cells. *Biochem Biophys Res Commun* 280:223-228.

Lee K, Tirasophon W, Shen X, Michalak M, Prywes R, Okada T, Yoshida H, Mori K, Kaufman RJ. (2002) IRE1-mediated unconventional mRNA splicing and S2P-mediated ATF6 cleavage merge to regulate XBP1 in signaling the unfolded protein response. *Genes Dev* 16:452-466.

Lotharius J., Dugan L.L., O'Malley K.L. (1999) Distinct mechanisms underlie neurotoxin-induced cell death in cultured dopaminergic neurons. J. Neurosci. 19: 1284-1293.

Ma Y, Hendershot LM. (2001) The unfolding tale of the unfolded protein response. Cell 107:827-30.

Oh Y.J., Wong S.C., Moffat M., O'Malley K.L. (1995) Overexpression of Bcl-2 attenuates MPP+, but not 6-OHDA-induced cell death in a dopaminergic neuronal cell line. Neurobiol. Dis. 2: 157-167.

O'Malley KL, Liu J, Lotharius J, Holtz W. (2003) Targeted expression of BCL-2 attenuates MPP(+) but not 6-OHDA induced cell death in dopaminergic neurons. Neurobiol Dis. 14:43-51.

Pan Y, Chen H, Siu F, Kilberg MS. (2003) Amino acid deprivation and endoplasmic reticulum stress induce expression of multiple activating transcription factor-3 mRNA species that, when overexpressed in HepG2 cells, modulate transcription by the human asparagine synthetase promoter. *J Biol Chem* 278:38402-38412.

Reimertz C, Kogel D, Rami A, Chittenden T, Prehn JH. (2003) Gene expression during ER stress-induced apoptosis in neurons: induction of the BH3-only protein Bbc3/PUMA and activation of the mitochondrial apoptosis pathway. J Cell Biol. 162:587-97.

Salinas M, Diaz R, Abraham NG, Ruiz de Galarreta CM, Cuadrado A. (2003) Nerve growth factor protects against 6-hydroxydopamine-induced oxidative stress by increasing expression of heme oxygenase-1 in a phosphatidylinositol 3-kinase-dependent manner. *J Biol Chem* 278:13898-13904.

Schèagger H, von Jagow G. (1991) Blue native electrophoresis for isolation of membrane protein complexes in enzymatically active form. *Anal Biochem* 199:223-231.

Schipper HM, Liberman A, Stopa EG. (1998) Neural heme oxygenase-1 expression in idiopathic Parkinson's disease. *Exp Neurol* 150:60-68.

Sherman MY, Goldberg AL. (2001) Cellular defenses against unfolded proteins: a cell biologist thinks about neurodegenerative diseases. Neuron 29:15-32.

Zatloukal K, Stumptner C, Fuchsbichler A, Heid H, Schnoelzer M, Kenner L, Kleinert R, Prinz M, Aguzzi A, Denk H. (2002) p62 is a common component of cytoplasmic inclusions in protein aggregation diseases. *Am J Pathol* 160:255-263.